ACS OMEGA

Open Access

http://pubs.acs.org/journal/acsodf

Article

Synthesis of a Novel Dithiocarbamate Surfactant Derivative Adsorbent for Efficient Removal of Heavy Metal Ions

Xingmin Wang,* Feilan Qi, Jie Xiong, Jujiao Zhao, Guizhi Zhang, Shahzad Afzal, Xingxing Gu, Qiudong Li, Shiyang Luo, and Hongbo Mo

Cite This: *ACS Omega* 2023, 8, 41512−41522

Read Online

ACCESS | Metrics & More | Article Recommendations

ABSTRACT: In this work, a novel heavy metal chelating agent (DTC-SDS) containing dithiocarbamate (DTC) was synthesized using sodium dodecyl sulfate (SDS), formaldehyde, and carbon disulfide. DTC-SDS has excellent trapping performance under pH 1−7 and initial concentrations 100−500 mg/L. With the increase in adsorbent dose, the adsorption amount of DTC-SDS increases and then decreases, and the optimized dosage of DTC-SDS is 0.02 g. The DTC-SDS adsorbent exhibits superior adsorption capacity (191.01, 111.7, and 79.14 mg/g) and high removal rates (97.99%, 98.48%, and 99.91%) for Mn^{2+}, Zn^{2+}, and Pb^{2+} respectively, in wastewater. Such remarkable adsorption performance could be attributed to the strong trapping effect on heavy metal ions by the C−S bond of DTC-SDS. The liquid adsorbent was in full contact with heavy metal ions, which further enhanced the complexation of heavy metal ions. The adsorption isothermal model showed that the adsorption process was typical of Langmuir monomolecular layer adsorption. Kinetic studies showed that the pseudo-second-order kinetic model fits the experimental adsorption data better than the pseudo-first-order kinetic model. In the ternary metal species system (Mn^{2+}, Zn^{2+}, and Pb^{2+}), DTC-SDS preferentially adsorbed Pb^{2+} due to its highest covalent index. The main controlling step is the chemical interaction between the active groups of DTC-SDS and the heavy metal ions. This work provides valuable insights into the adsorption of heavy metal ions onto dithiocarbamate, which could guide the development of other heavy metal chelating agents and be beneficial for developing novel treatments of wastewater contaminated with heavy metals.

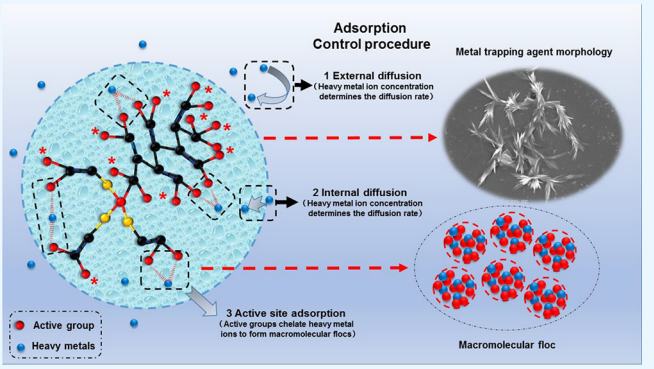

1. INTRODUCTION

The heavy metal mass concentration exceeding the allowable environmental value will cause significant damage to the ecological environment and seriously endanger human health.[1] Typical toxic heavy metals in polluted water include manganese, zinc, lead, etc.[2] For example, high concentrations of Mn can affect hepatic, vascular, immune, and reproductive systems;[3] Zn can lead to vomiting, diarrhea, gastric perforation, intestinal necrosis, and even death by shock;[4] Pb can damage the renal, hepatic, reproductive, and brain nervous system.[5] Several technologies for the removal of heavy metals have been investigated extensively, such as chemical precipitation,[6] ion-exchange,[7] membrane filtration,[8] electrochemical treatment technologies, adsorption,[9] etc. Among these methods, chemical precipitation is widely used to treat wastewater with a relatively high concentration of heavy metals due to its high efficiency, easy handling, and low energy consumption. However, this method requires large doses and produces large amounts of sludge, increasing the difficulty of sludge treatment.[1] The adsorption method presents similar advantages while it could significantly reduce the production of sludge.[10] Nevertheless, most adsorbents are solid phase in that heterogeneous adsorption is slower than a homogeneous chemical reaction, resulting in relatively poor efficiency.[10] Therefore, novel soluble adsorbents that can capture heavy metals in the liquid phases are highly demanded.

The heavy metal chelating agent is an organic agent that contains specific functional groups that can chelate, trap, and precipitate heavy metal ions from wastewater.[11] Dithiocarbamates (DTCs) are one kind of heavy metal chelating agent. Based on the theory of hard and soft acids and bases (HSAB), DTCs, a soft base, could be used as selective adsorption material to remove heavy metal ions.[12] This method has

Received: July 27, 2023
Accepted: September 18, 2023
Published: October 25, 2023

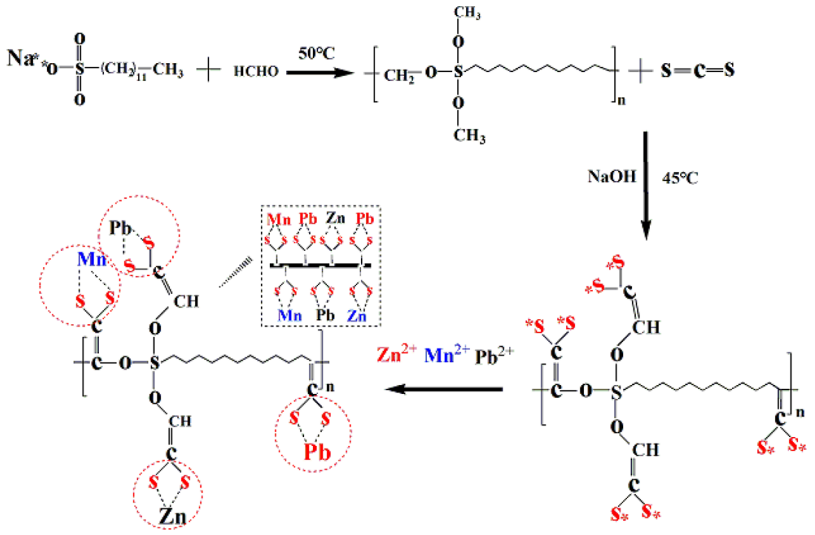

Figure 1. Synthesis process of DTC-SDS.

attracted much attention due to its fast reaction rate, stable precipitation products, and simple operation.[13] Tan et al. synthesized a heavy metal chelating agent having dithiocarboxyl groups with an adsorption capacity of 26.56 mg/g to remove Mn^{2+}.[14] Li et al. prepared DTC-MWCNT to remove complexed Zn^{2+} with an adsorption capacity of 11.2 mg/g.[15] Similarly, Li et al. synthesized DTC-LPEI with an adsorption capacity of 20.25 mg/g to remove Zn^{2+} at pH 5.5.[16] The above research focused on preparing small molecule DTCs, which have good water solubility and are effective in treating most simple or complex systems of heavy metal wastewater. However, the complex flocs with heavy metal ions are so small that the flocs settle slowly, and the resulting sludge is less dense, large in volume, and high in water content.

Large-molecule organosulfur DTCs have a larger molecular weight and contain more functional groups in the molecular chain, which perform better trapping than small-molecule DTCs. Moreover, it generates larger flocs with heavy metal ions that are easy to settle. However, because large molecule DTCs are usually synthesized by the reaction of organic amines and carbon disulfides, the molecular chain of DTCs contains a large number of carbon chains, leading to the poor water solubility of these DTCs.

Masafumi et al. reported that the reaction of polyethylenimine with carbon disulfide produced polymeric DTCs containing functional groups, although this polymeric heavy metal trap is insoluble in water.[17] The Carey team generated poly(DTCs) by reacting poly(dichloroethylene) or poly(polyethylenimine) with carbon disulfide. The water solubility of poly(DTCs) decreased when the molecular weight of poly ammonia increased.[17] For now, it is still important to explore novel methods that can synthesize water-soluble macromolecular DTCs.

Herein, an easily scale-up method was developed to synthesize DTCs with sodium dodecyl sulfate (SDS), which is the most commonly used and cheap surfactant.[18] By using SDS and carbon disulfide as raw materials and formaldehyde as the cross-linking agent, the obtained novel polymer DTCs, which is named DTC-SDS, are presented in the form of macromolecular with good water solubility. The DTC-SDS was used for the adsorption of Pb^{2+}, Mn^{2+}, and Zn^{2+}, and it exhibits excellent performance due to the significantly increasing numbers of C−S and a large amount of long molecular chains, which could reduce the spatial site resistance. The effects of the solution pH and DTC-SDS dosage were systematically investigated. The adsorption kinetics and adsorption diffusion model were discussed. Furthermore, the adsorption mechanism and the impact of DTC-SDS on the removal of heavy metal ions in the ternary system are also proposed.

2. MATERIALS AND METHODS

2.1. Materials and Characterizations. Sodium dodecyl sulfonate, formaldehyde, carbon disulfide, hydrochloric acid, and sodium hydroxide of analytical purity are purchased from China Chemical Reagent Network. Multielement mixed standard solution (Al, As, Cd, Cr, Cu, Ni, Pb, Mn, Cd, Zn) was purchased from Aladdin Corporation. The pH index was measured with a pH meter (Thunder Magnetic PHS-3C). The heavy metal ion concentrations were analyzed by an inductively coupled plasma atomic emission spectrometer (ICP-AES, SPECTRO GESISE). The ICP detection conditions were the following: plasma gas was 10−12 MPa, auxiliary gas was 0.6−0.8 MPa, carrier gas was 0.6−0.8 MPa, purge time was 120 s, tests number was 2, test time was 30 s, and the gas was argon. Fourier transform infrared spectroscopy (FT-IR Prestige-21) was used to determine the functional groups, and FT-IR was in the attenuated total reflection mode, and the measured wavenumber was 4000−500 cm^{-1}. A scanning electron microscope (SU-1510) was used to measure the apparent morphology, and the working voltage was 15 kV. Aqueous gel permeation chromatography (GPC, Agilent PL-GPC50) was used to measure the molecular mass of the compounds to calculate the degree of product polymerization. The X-ray photoelectron spectroscopy (XPS) tests were carried out with a Thermo Scientific K-Alpha spectrometer with a monochromatic Al Kα source (1486.6 eV). All of the reported binding energies were corrected for charging effects by the C 1s peak (284.8 eV) of adventitious carbon on the analyzed sample surface.

2.2. Preparation of DTC-SDS by Graft Polymerization. DTC-SDS was prepared by graft polymerization as shown in Figure 1.[19] At 50 °C, 1 mmol of sodium dodecyl sulfate (SDS) was added to 25 mL of deionized water. After stirring for half

https://doi.org/10.1021/acsomega.3c05476
ACS Omega 2023, 8, 41512−41522

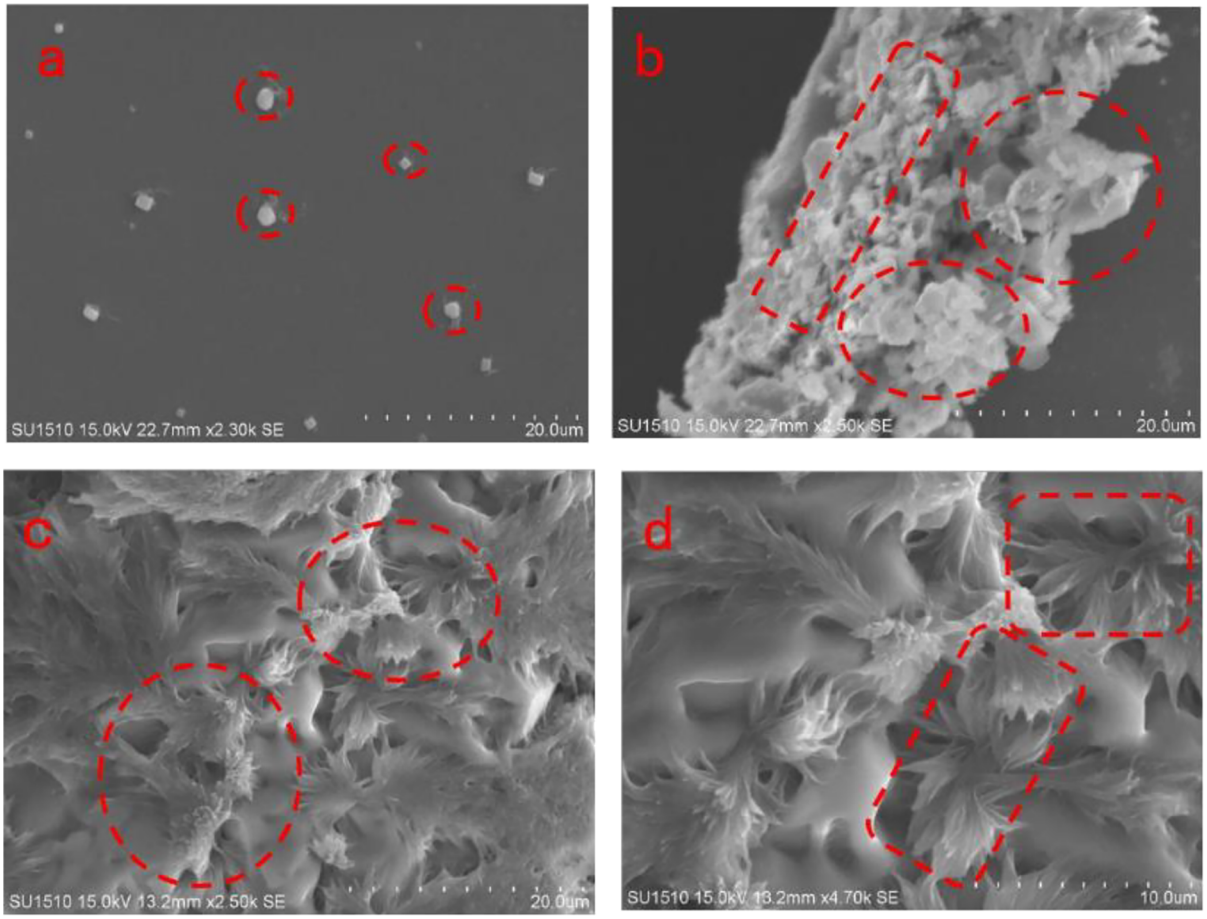

Figure 2. SEM images of (a) SDS, (b)(c)(d) DTC-SDS.

an hour, 3 mmol of formaldehyde is added to the SDS solution. The mixture is stirred for 1 h and cooled to room temperature. Then, 4 mmol of the chelating group donor CS_2 and 0.1 mmol of the cross-linking agent NaOH are added. The reaction is carried out at room temperature for 1 h. A pale yellow liquid is finally obtained.

2.3. Preparation of Heavy Metal Ion Solution. A standard mixed sample with a mass concentration of 100 mg/L is taken in a volumetric flask and diluted into different standard solutions with 0, 0.1, 1, 5, and 10 mg/L. The intensities are measured under the set working conditions of ICP-AES, and the standard curves are plotted.

2.4. Adsorption Experiment. The effect of pH on the adsorption of the metal ions is studied at 25 °C. A series of 50 mL flasks are used. 0.04 g of DTC-SDS and 50.0 mL of metal ions (200 mg/L) are added to each flask. The desired pH is adjusted using an aqueous solution of each HCl and NaOH (0.1 mol/L). A pH range of 1.0 to 7.0 was used to avoid the precipitation of metal hydroxides. The flask was shaken in the thermostat shaker for 60 min. After resting, the supernatant is filtered through a 0.45 μm filter membrane. The residual concentration of each metal ion is determined by ICP-AES to calculate the adsorption capacities of metal ions according to eqs 1−3:

$$Y = \frac{c_0 - c_t}{c_0} \times 100\% \tag{1}$$

$$q_t = \frac{(c_0 - c_t)V}{m} \tag{2}$$

$$q_e = \frac{(c_0 - c_e)V}{m} \tag{3}$$

Y is the removal rate, q_t is the amount of heavy metal ions adsorbed per unit mass of adsorbent at equilibrium, and the equilibrium removal amount q_e is calculated as follows: the c_0 (mg/L) is the initial mass concentration of the target metal ion in the wastewater sample; c_t (mg/L) is the mass concentration of the metal ion after a certain adsorption contact time; c_e (mg/L) is the mass concentration of the metal ion at the adsorption equilibrium; m (g) represents the mass of the metal trapping agent; V (L) is the volume of the wastewater sample.

For the kinetic adsorption, 0.05 g of DTC-SDS is weighed into the flasks with 50.0 mL of metal ions solution at 200 mg/L. The pH was kept at 7 throughout kinetic studies. The flasks were agitated for 500 min at 25 °C in a shaking thermostatic bath. The concentration of each metal ion was measured at different time intervals of up to 500 min. The calculation formulas of the kinetic model are shown in eqs 4 and 5:

$$\log(q_e - q_t) = \log q_e - k_1 t \tag{4}$$

$$\frac{t}{q_t} = \frac{1}{K_2 q_e^2} + \frac{t}{q_e} \tag{5}$$

https://doi.org/10.1021/acsomega.3c05476
ACS Omega 2023, 8, 41512−41522

where k_1 (min^{-1}) is the quasi-first order reaction rate constant and k_2 [(g mg^{-1}) min^{-1}] is the rate constant of the quasi-second-order reaction.

The diffusion model is calculated by the following equations:

$$q_t = k_i t^{1/2} + c \quad (6)$$

$$\log(1 - F) = - k_f t \quad (7)$$

where F is the balance proximity coefficient, k_f (min^{-1}) is the external diffusion rate constant, k_i [mg/(g $min^{0.5}$)] is the internal diffusion rate constant, and c (mg/g) is the intercept of the internal diffusion curve.

The degree of polymerization (Dp) is calculated by the following equations:

$$\mathrm{Dp} = \mathrm{Mn} \div M_0 \quad (8)$$

where Mn is the number-average relative molecular mass, which was measured by GPC and is 168223 and M_0 is 557, which is the repeat group molecular mass of DTC-SDS.

The Langmuir adsorption isothermal model is calculated by the following equations:

$$\frac{1}{q_t} = \frac{1}{ab} \times \frac{1}{c_0} + \frac{1}{b} \quad (9)$$

where a and b are constant (math.).

3. RESULTS AND DISCUSSION

3.1. Material Characterization. *3.1.1. SEM Images.* The morphologies and structures of SDS and DTC-SDS were characterized. As depicted, SDS presents a homogeneous granular form (Figure 2a). In Figure 2b, the DTC-SDS particles are observed to agglomerate together as a result of cross-linking. The surface of DTC-SDS particles partly collapses because of the structure damage by NaOH during the preparation process. As shown in Figure 2c,d, further zoomed-in view, the surface of the DTC-SDS shows a flowerlike structure with abundant micropores. The surface has massive depressed areas and abundant pores with ions accommodation space. The irregular DTC-SDS particles have a rough and loose surface, providing a good possibility for trapping heavy metal ions.[20]

3.1.2. FT-IR Spectrum. The FT-IR spectra of the DTC-SDS sample, SDS, and CS_2 are shown in Figure 3. As can be seen in Figure 3, the DTC-SDS has three characteristic peaks. The peak at around 1640 cm^{-1} is mainly due to the bending vibration of the C−S bond of the DTC-SDS.[21] A broad absorption band at 3433 cm^{-1} is usually assigned to the O−H of the adsorbed water.[22] The peak at 1400 cm^{-1} is attributed to the C−O bending vibration.[23,24] These results verify the presence of C−S in the DTC-SDS groups.

3.1.3. GPC Test. The relative molecular masses of DTC-SDS are measured by GPC and the degree of polymerization is calculated. DTC-SDS presents an average relative molecular mass of 168463, which means that the degree of polymerization of DTC-SDS is 302.

3.2. Adsorption Performance. *3.2.1. Effect of pH.* The pH of the aqueous solution is an important controlling parameter in the heavy metal ion adsorption process. This study investigates the removal of heavy metals (Mn^{2+}, Zn^{2+}, and Pb^{2+}) by DTC-SDS at the initial pH range of 1 to 7 at 25 °C. As shown in Figure 4, the removal amount of heavy metals enhances with the pH increase. The adsorption of Mn^{2+}

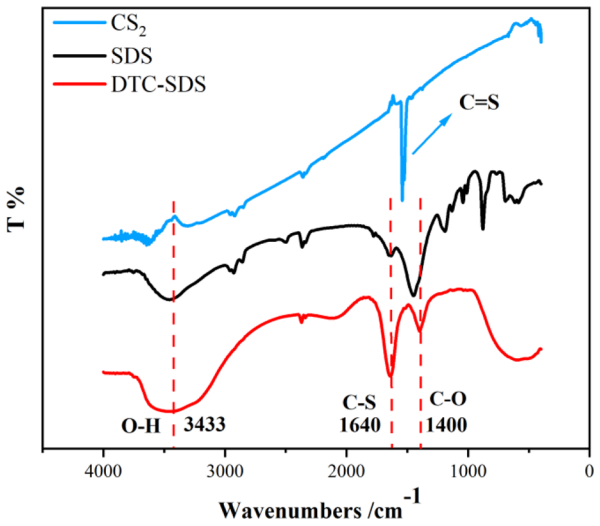

Figure 3. FT-IR spectra of DTC-SDS, SDS, and CS_2.

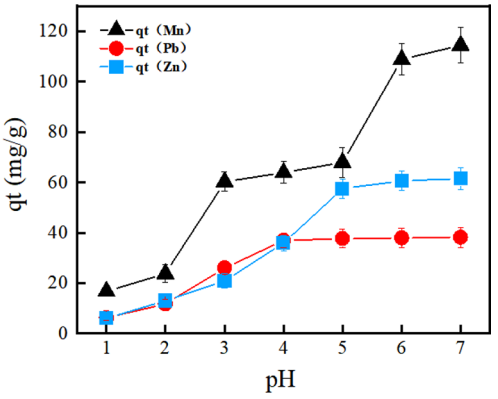

Figure 4. Effect of solution pH on the removal of heavy metal ions by DTC-SDS (concentration of heavy metal ions, 200 mg/L; solution volume, 50.0 mL; DTC-SDS, 0.04 g; temperature, 25 ± 1 °C; reaction time, 60 min).

increases with increasing pH, with a maximum capacity of 114.5 mg/g at around pH 7. At pH 5−7, the maximum adsorption removal of Zn^{2+} is 61.4 mg/g. At pH 4−7, the adsorption capacity of Pb^{2+} is more than 30 mg/g. However, at pH 1, the adsorption capacity of DTC-SDS for heavy metal ions is less than 20 mg/g. The poor performance of DTC-SDS at strong acidic conditions (pH < 2) is due to abundant H^+, protonating the active groups of the metal trapping agent, reducing the ionization degree of the groups, as well as the active sites that bind to metal ions.[25,26] That is, S, which contains a lone pair of electrons, can act as a proton acceptor that binds an H^+ through a coordination bond to form S^+. Therefore, the C−S on the DTC-SDS prefers to chelate with hydrogen ions rather than heavy metal ions due to the protonation.[27,28] In addition, the strong acid environment will destroy the structural integrity of the DTC-SDS and increase its solubility, resulting in the difficulty of DTC-SDS to form stable macromolecular compounds with heavy metal ions.[29,30] In conclusion, DTC-SDS has excellent trapping performance under acidic conditions and is suitable for a wide range of acid-complexed heavy metal wastewater.

3.2.2. Dosage of DTC-SDS. The effect of the adsorbent dose on the removal of heavy metal ions is shown in Figure 5. The DTC-SDS exhibits superior adsorption capacity (191.01,

https://doi.org/10.1021/acsomega.3c05476
ACS Omega 2023, 8, 41512−41522

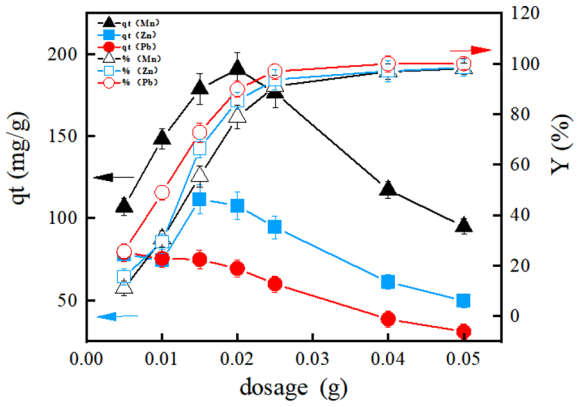

Figure 5. Effect of DTC-SDS dosage for the removal of heavy metal ions (concentration of heavy metal ions, 200 mg/L; solution volume, 50.0 mL; temperature, 25 ± 1 °C; reaction time, 60 min; pH = 7).

111.7, and 79.14 mg/g) and high removal rates (97.99%, 98.48%, and 99.91%) for Mn^{2+}, Zn^{2+}, and Pb^{2+} in wastewater, respectively. The removal percentage increases rapidly with the increase in adsorbent dose at the beginning. The removal percentage reaches an almost constant value at the critical adsorbent dose (around 0.05 g). However, the amount of heavy metal ions adsorbed per unit mass of DTC-SDS at equilibrium show a mountain-shaped trend that first increases and then decreases. Because when the number of active sites provided by the metal trapping agent is greater than the content of metal ions, overlapping of active sites will occur, resulting in a decrease in the utilization efficiency of active groups.[31,32] Thus, the optimized dosage of DTC-SDS is 0.02 g.

The adsorption capacities q_t for different types of adsorbents used in the removal of heavy metal ions are compared in Table 1. As shown in Table 1, the maximum adsorption capacities of DTC-SDS are higher than those of many other reported adsorbents, and the equilibrium time is short, suggesting that DTC-SDS is an effective adsorbent for removing heavy metal ions.

3.2.3. Initial Concentration of Heavy Metal Ions. The mass concentration of heavy metal ions can affect the initial kinetic energy of DTC-SDS during the removal of heavy metal ions. When the dosage of DTC-SDS was 0.02 g and other conditions were the same as 3.2.2, the effects of Mn^{2+}, Zn^{2+}, and Pb^{2+} mass concentrations of 100−500 mg/L on the performance of DTC-SDS were investigated. From Figure 6a, it can be seen that the adsorption amount of Mn^{2+}, Zn^{2+}, and Pb^{2+} by DTC-SDS increased with the increase in mass concentration. At a mass concentration of 400 mg/L, the removal of Zn^{2+} and Pb^{2+} was saturated with the amounts of 227.64 and 119.41 mg/g. At a mass concentration of 500 mg/L, the removal of Mn^{2+} was saturated with a concentration of 406.53 mg/g. The saturated adsorption amount of DTC-SDS was Mn^{2+} > Zn^{2+} > Pb^{2+}. In addition, we fitted the adsorption isothermal model, as shown in Figure 6b. The adsorption process of Mn^{2+}, Zn^{2+}, and Pb^{2+} by DTC-SDS was typical of Langmuir monomolecular layer adsorption with R^2 are 0.9962, 0.9982, and 0.9761, respectively.

3.3. Analysis of Adsorption Kinetic Models. The parameters of the three kinetic equations are shown in Table 2. The correlation coefficients of the pseudo-second-order equation (R^2 = 0.9999) are higher than those obtained from the pseudo-first-order equation (R^2 = 0.9414−0.9978). Therefore, the adsorption behavior of Mn^{2+}, Zn^{2+}, and Pb^{2+} onto DTC-SDS fit well with the pseudo-second-order equation. In addition, good agreement with this kinetic adsorption model is confirmed by the fact that the experimental equilibrium removal amount ($q_{e,exp}$), are closer to the calculated values, ($q_{e,cal}$). Figure 7a shows that the quasi-first-order model can describe only the initial phase of heavy metal ion removal by DTC-SDS and cannot describe the entire removal process. Therefore, the adsorption time is only 100 min. Figure 7b shows that the pseudo-second-order model curves are linear when the temperature is set at 298.15 K. It demonstrates that the chemisorption is the rate-controlling step,[37,38] and the main driving force is the chemical interaction process between the active groups of the metal trapping agent and the metal ions.[39,40]

3.4. Diffusion Model Analysis. The parameters of the diffusion model equations are shown in Table 3. The correlation coefficients of the external diffusion model (R^2 = 0.9414−0.9978) and the internal diffusion model (R^2 = 0.9631−0.9747) both fit well. Figure 8a,b also shows that the internal and external diffusion model curves are linear. It indicates that the diffusion of metal ions from the solution to DTC-SDS includes two stages. The initial stage is external diffusion. The external diffusion rate constant k_f is Pb^{2+} (0.1368) > Mn^{2+} (0.0324) > Zn^{2+} (0.0309). It indicates that Pb^{2+} is diffused more easily from the solution to the outer surface of DTC-SDS during the external diffusion phase. The second stage is internal diffusion. The internal diffusion rate constant k_i Mn^{2+}(1.4436) > Pb^{2+} (0.6258) > Zn^{2+} (0.6125), indicating that Mn^{2+} is diffused more easily from the surface of DTC-SDS to the inside of DTC-SDS. This may be the reason for the maximum adsorption and the fastest rate of Mn^{2+} adsorption by DTC-SDS in a single solution. Both stages are driven by the difference in the concentration of heavy metal

Table 1. Comparison of the Chemical Precipitation for the Removal of Heavy Metal Ions from Water

adsorbent	heavy metal ions	initial concentration (mg/L)	dose (g)	pH	capacity (mg/g)	equilibrium time (min)	temperature (°C)	references
DTC-SDS	$Mn^{2+}Zn^{2+}Pb^{2+}$	200	0.050.040.01	7	191.01111.7079.14	60	25	this work
active carbon	Pb^{2+}	1	4	6	1.295	120	20	33
natural bentonite	Zn^{2+}	300			52.91			33
resin	Pb^{2+}	40	2	5	19.64	180		34
fly ash	Pb^{2+}	30	5	6	5.91	90	20	35
zeolite	$Cu^{2+}Pb^{2+}$	200	4	6	4549	3045	20	36
DTCs	Mn^{2+}	100	3.5	6	26.56			14
DTC-MWCNT	$Cu^{2+}Zn^{2+}$	10	5	6	98.1 11.2	120	25	15
DTC-LPEI	$Cu^{2+}Zn^{2+}$	100	4	5.5	24.6520.25	2880	25	16

https://doi.org/10.1021/acsomega.3c05476
ACS Omega 2023, 8, 41512−41522

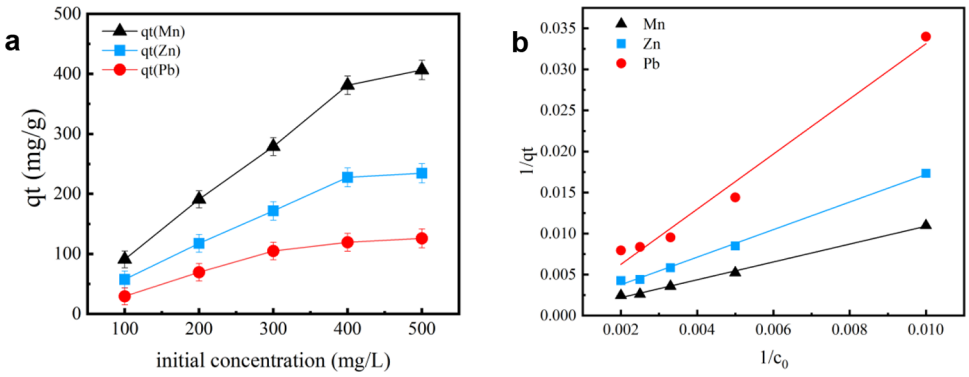

Figure 6. (a) Effect of initial concentration of heavy metal ions, (b) isotherm model (solution volume, 50.0 mL; DTC-SDS, 0.02 g; temperature, 25 ± 1 °C; reaction time, 60 min; pH = 7).

Table 2. Kinetic Results

			pseudo-first-order			pseudo-second-order		
metal ion	C_0/(mg g^{-1})	$q_{e,exp}$/(mg g^{-1})	$q_{e,c}$/(mg g^{-1})	k_1 /(min^{-1})	R^2	$q_{e,c}$ /(mg g^{-1})	k_2 /[(g mg^{-1}) min^{-1}]	R^2
Mn	455.45	111.45	9.45	0.0324	0.9617	111.11	0.0198	0.9999
Zn	248.63	61.22	4.24	0.0309	0.9978	61.35	0.0380	0.9999
Pb	156.88	39.18	3.80	0.1368	0.9414	39.22	0.0217	0.9999

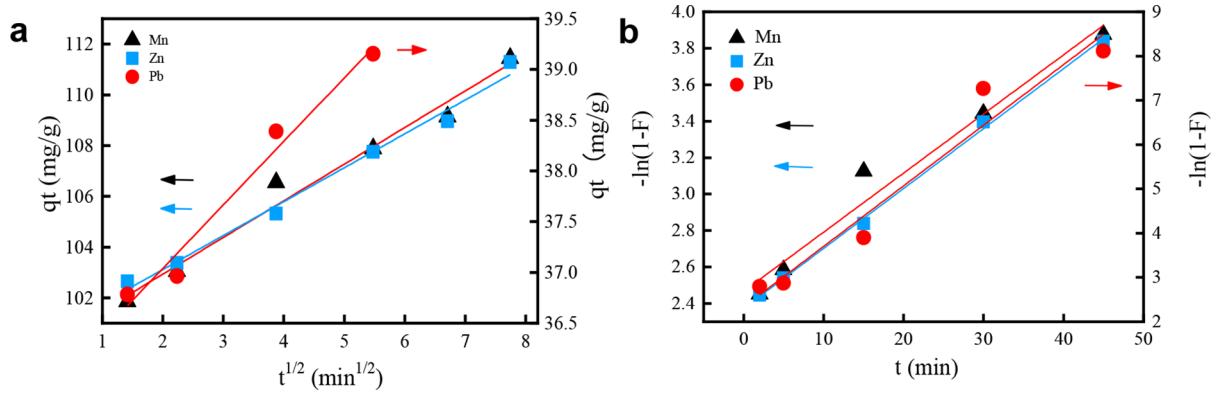

Figure 7. (a) Pseudo-first-order kinetic model linear fitting. (b) Pseudo-second-order kinetic adsorption (concentration of heavy metal ions, 200 mg/L; solution volume, 50.0 mL; temperature, 25 ± 1 °C; DTC-SDS amount, 0.02 g, pH = 7).

Table 3. Diffusion Model Parameters of DTC-SDS

	internal diffusion model			external diffusion model		
metal ion	C /(mg g^{-1})	K_i /[mg/(g $min^{0.5}$)]	R^2	intercept	K_f/(min^{-1})	R^2
Mn	100.05	1.4436	0.9747	2.4671	0.0324	0.9617
Zn	56.25	0.6125	0.9859	2.6691	0.0309	0.9978
Pb	35.79	0.6258	0.9631	2.3334	0.1368	0.9414

ions.[41,42] Regarding why Pb^{2+} diffuses more easily to the outer surface and Mn^{2+} diffuses more easily to the interior, much literature has been reviewed; however, the phenomenon cannot be clearly explained yet, and the reason will be investigated afterward.

3.5. Competitive Adsorption of Heavy Metal Ions. The competitive adsorption capacity of DTC-SDS in the ternary metal species system is investigated. As shown in Figure 9, the equilibrium adsorption amounts of Pb^{2+}, Mn^{2+}, and Zn^{2+} are all reduced in the ternary system compared to single heavy metal ion adsorption. Additionally, in a single system, the equilibrium adsorption is $Mn^{2+} > Zn^{2+} > Pb^{2+}$. This is due to the easier diffusion of Mn^{2+} from the surface of DTC-SDS to the inside of DTC-SDS. In ternary systems, the equilibrium adsorption is $Pb^{2+} > Zn^{2+} > Mn^{2+}$. The preferential adsorption of Pb^{2+} greatly reduces the adsorption amounts of Mn^{2+} and Zn^{2+}. However, the adsorption of Pb^{2+} is less influenced by Mn^{2+} and Zn^{2+}, while the adsorption amounts of Mn^{2+} vary the most. These results indicate that DTC-SDS is suitable for the preferential adsorption of Pb^{2+} in multiple heavy metal ion solutions.

The origin of the selective adsorption of Pb^{2+} in ternary systems is further discussed. The equilibrium adsorption amounts of heavy metal ions are correlated with some factors, such as electronegative, atomic number, ionic potential, and ionic radius, etc. Because it is difficult to order the heavy metal ions based on a single factor as described above, a concept of the covalent index is proposed by Nieboer and Richardson-

https://doi.org/10.1021/acsomega.3c05476
ACS Omega 2023, 8, 41512−41522

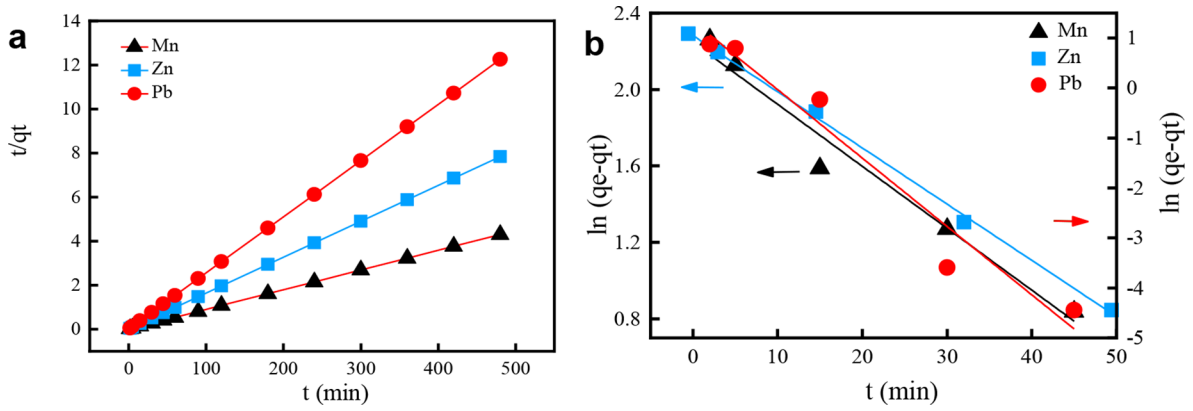

Figure 8. (a) Linear fitting of external diffusion model and (b) linear fitting of internal diffusion model (concentration of heavy metal ions, 200 mg/L; solution volume, 50.0 mL; temperature, 25 ± 1 °C, DTC-SDS amount, 0.02 g, pH = 7).

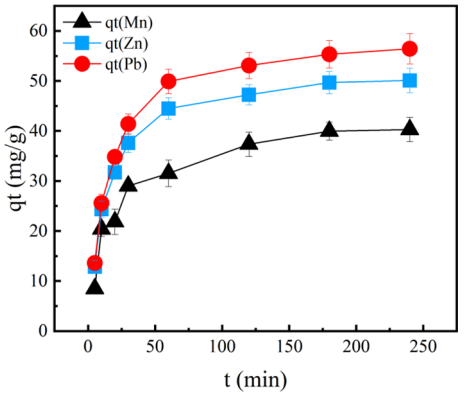

Figure 9. Kinetics of competitive adsorption of heavy metal ions(concentration of heavy metal ions, 200 mg/L; solution volume, 50.0 mL; temperature, 25 ± 1 °C; DTC-SDS amount, 0.02 g, pH = 7).

(HSAB theory).[43] The covalent index is a parameter computed using the following expression: $X_m^2 r$, where X_m is electronegativity and r is ionic radius.[44] X_m^2r is an index of metal–ligand complex stability in an aqueous solution involving metal ions. The larger the covalent index, the more stable the covalent bonds formed between the metal ions and DTC-SDS. The covalent indices of the three heavy metals are ranked as follows: Pb^{2+} (3.41) > Zn^{2+} (2.04) > Mn^{2+} (1.94), which is the same as the order observed from the adsorption experiments with DTC-SDS as adsorbents in ternary systems. Thus, these results further demonstrate that the good adsorption performance of DTC-SDS originates from the formation of the metal–ligand complex, and the preferential adsorption of Pb^{2+} can be attributed to the higher covalent bonding ability of Pb^{2+}.

3.6. Analysis of the Adsorption Mechanism. As seen from Figure 10, the adsorption process is divided into three stages: (1) External diffusion stage. Heavy metal ions rapidly transport onto the surface of DTC-SDS; (2) Internal diffusion stage. Heavy metal ions diffuse to the inside of DTC-SDS; (3) Active site adsorption. This is the rate-limiting step and the final equilibrium step due to the lower concentration of heavy metal ions in the aqueous solution. Stage 1 and stage 2 are physical processes, and stage 3 is a chemical process.[44,45]

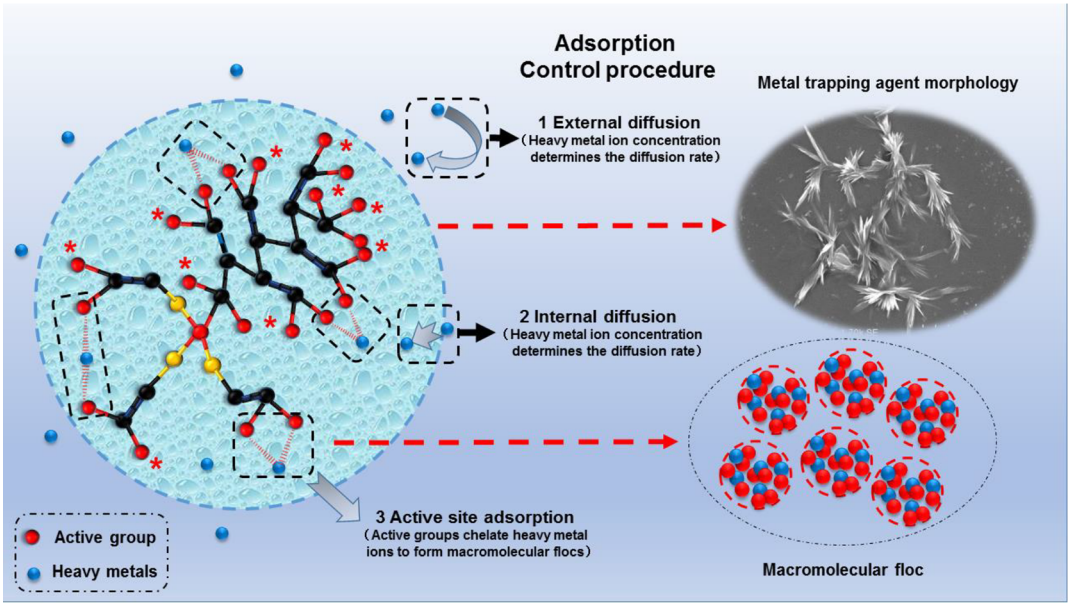

Figure 10. Analysis of the process of DTC-SDS to remove heavy metal ions.

https://doi.org/10.1021/acsomega.3c05476
ACS Omega 2023, 8, 41512−41522

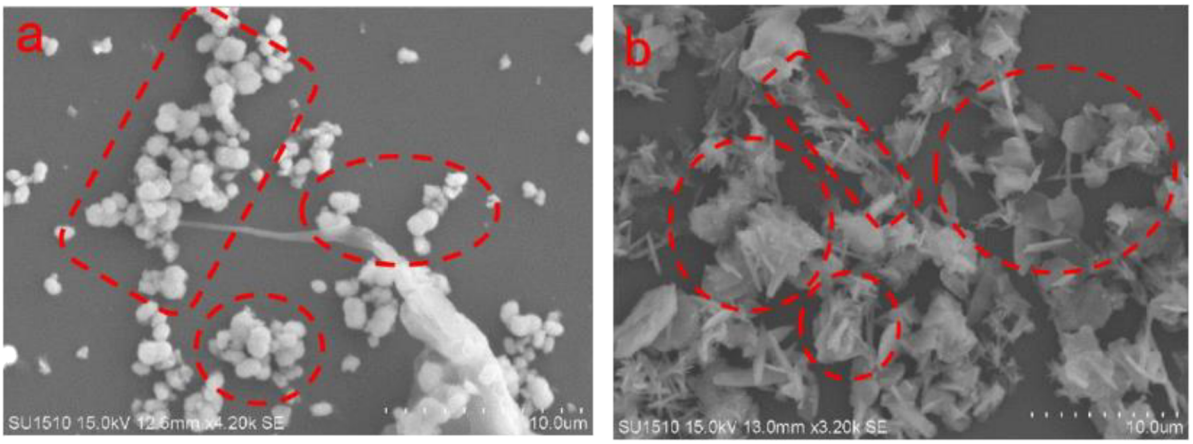

Figure 11. SEM images of precipitates (a) in the single heavy metal ion solution and (b) in the ternary solution.

DTC-SDS uses S-atoms in the polar groups of the structure to trap heavy metal ions, which then generate chemical bonds to produce insoluble covalent chelates, forming a quaternary ring with a heavy metal core.[46] The spatial assignment of the electron-giving group around the central ion plays a decisive role in the angle of the bonding orbital assignment of the metal ion.[47] For example, Zn has an electronic structure of $3d^{10}4s^2$ and loses two electrons from the 4s orbital to form a zinc ion. When reacting with DTC-SDS, the 3d orbital of the zinc ion is saturated and therefore forms an sp^3 orbital with a positive tetrahedral configuration and a central ion coordination number of 4.[48] The trapping agent combines with metal ions with dsp^2, sp^3, and d^2sp^3 valence bonding orbitals to form different spatial structures such as ortho-tetrahedra and ortho-octahedra to produce insoluble chelated precipitates for the separation of heavy metals in wastewater.[49]

Figure 11 presents the SEM images of the precipitates. Figure 11a shows the precipitates of DTC-SDS in the single heavy metal ion solution, and Figure 11b shows the precipitates in the ternary solution. The precipitates are dispersed macromolecular particles and formed large complexes. The difference in the morphology of the two precipitates may be due to DTC-SDS forming a larger precipitate in the ternary solution.

Figure 12 shows the FT-IR spectrum of DTC-SDS-Mn, Zn, and Pb after adsorption. Compared with the FT-IR spectrum of DTC-SDS, the absorption peak of the stretching vibration of the C−S bond is displaced from 1640 to 1377 cm^{-1} with decreased intensity. This may be because that when C−S, the main group of DTC-SDS, chelates with Mn, Zn, and Pb, the S atoms form coordination bonds through the lone pair of electrons, the electronegativity of the S atoms decreases, and the conjugation system of C−S is changed, thus causing changes in the peaks.[50] Meanwhile, the C−O vibrational stretching peak also shifts from 1400 to 1124 cm^{-1}. These results could be attributed to the formation of coordination bonds between S atoms and heavy metal ions, indicating the S sites of C−S bonds play an important role in good adsorption performance.

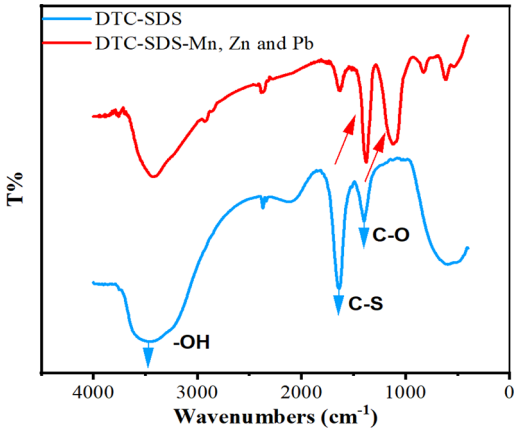

Figure 12. FT-IR spectra of DTC-SDS and DTC-SDS-Mn, Zn, and Pb.

The chemical composition of the precipitates obtained after the adsorption in the ternary solution is investigated by XPS. As illustrated in Figure 13a, the signals of C, S, O, Mn, Zn, and Pb are present in the XPS survey spectra of DTC-SDS. High-resolution XPS spectra of S 2p (Figure 13b) can be deconvoluted into three peaks (162.38, 166.38, and 169.08 eV), corresponding to S−Pb, S−Mn, and S−Zn, respectively.[50,51] The Mn 2p spectrum (Figure 13c) reveals the existence of Mn−S $2p_{1/2}$ and $2p_{3/2}$ located at 643.38, and 654.58 eV, respectively.[52] The Zn 2p spectra (Figure 13d) contains two peaks located at 1022.08 and 1045.08 eV corresponding to Zn $2p_{1/2}$ and Zn $2p_{3/2}$, respectively.[53] The peaks at 138.78 and 143.68 eV are attributed to Pb 4f (Figure 13e).[50] The above results indicate that DTC-SDS traps heavy metals mainly through the S sites of C−S bonds because of the coordination interaction between S and heavy metal ions. The results are in general agreement with the results from FT-IR spectroscopy.

4. CONCLUSIONS

In conclusion, DTC-SDS was successfully synthesized via the graft polymerization method, and the C−S bond was grafted onto the SDS skeleton. It was then used as an effective adsorbent in the removal of heavy metal ions. The results showed that the DTC-SDS has a high adsorption capacity on Mn^{2+}, Zn^{2+}, and Pb^{2+} with significantly high removal rates of 97.99%, 98.48%, and 99.91%, respectively. The adsorption capacity of DTC-SDS was influenced by pH and dosage, with the optimized pH and dosage being 7 and 0.02 g, respectively. In addition, the adsorption isothermal model showed that the adsorption process was typical of Langmuir monomolecular layer adsorption, and the kinetic data fitted well with the

https://doi.org/10.1021/acsomega.3c05476
ACS Omega 2023, 8, 41512−41522

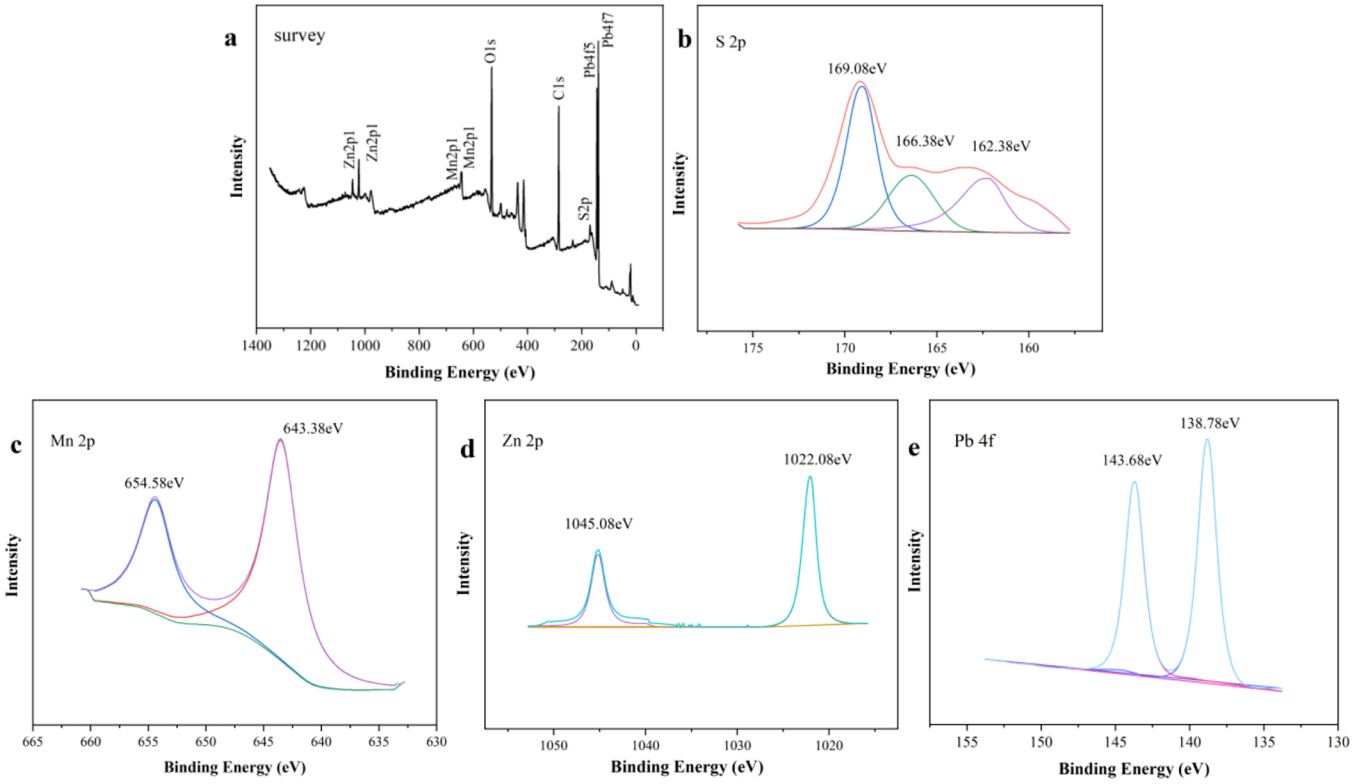

Figure 13. XPS survey scan of DTC-SDS treated with heavy metal: (a) survey spectrum, (b) S 2p, (c)Mn 2p, (d)Zn 2p, and (e)Pb 4f.

pseudo-second-order kinetic model. The removal of metal ions in wastewater by DTC-SDS is mainly based on the chemical interaction between the C−S active groups and metal ions. In mixed solutions, DTC-SDS preferentially adsorbed Pb^{2+}, and the selective adsorption was mainly attributed to the difference in the covalent index of the heavy metal ions. DTC-SDS is suitable for the preferential adsorption of Pb^{2+} in multiple heavy metal ion solutions.

AUTHOR INFORMATION

Corresponding Author

Xingmin Wang − *School of Environment and Resources, Chongqing Technology and Business University, Chongqing 400067, P.R. China;* orcid.org/0000-0002-9753-2956; Email: wxm0826@ctbu.edu.cn

Authors

Feilan Qi − *School of Environment and Resources, Chongqing Technology and Business University, Chongqing 400067, P.R. China*

Jie Xiong − *School of Environment and Resources, Chongqing Technology and Business University, Chongqing 400067, P.R. China*

Jujiao Zhao − *School of Environment and Resources, Chongqing Technology and Business University, Chongqing 400067, P.R. China*

Guizhi Zhang − *School of Environment and Resources, Chongqing Technology and Business University, Chongqing 400067, P.R. China*

Shahzad Afzal − *Department of Environmental Engineering, China Jiliang University, Hangzhou, Zhejiang 310018, P.R. China*

Xingxing Gu − *School of Environment and Resources, Chongqing Technology and Business University, Chongqing 400067, P.R. China;* orcid.org/0000-0002-5145-7751

Qiudong Li − *School of Environment and Resources, Chongqing Technology and Business University, Chongqing 400067, P.R. China*

Shiyang Luo − *School of Environment and Resources, Chongqing Technology and Business University, Chongqing 400067, P.R. China*

Hongbo Mo − *Chongqing Academy of Metrology and Quality Inspection Chongqing, Chongqing, CN 400047, China*

Complete contact information is available at: https://pubs.acs.org/10.1021/acsomega.3c05476

Author Contributions

X.W.: conceptualization, supervision, project administration, funding acquisition, writing−review and editing. F.Q.: methodology, investigation, validation, writing−original draft. J.X.: methodology, investigation, validation, writing−original draft. J.Z.: funding acquisition, writing−review and editing. G.Z.: methodology, investigation. S.A.: writing−review and editing. X.G.: writing−review and editing, methodology. Q.L.: validation. S.L.: validation. H.M.: review & editing.

Notes

The authors declare no competing financial interest.

The authors declare that this study did not involve experiments on human tissue.

ACKNOWLEDGMENTS

This research was supported by the Humanities and Social Sciences Youth Foundation, Ministry of Education of the People's Republic of China(Nos. 13JYCZH185), and Chongq-

ing Talent Program "Package" Project (Nos. cstc2022ycjh-bgzxm0176). Shahzad Afzal Hongbo Mo

REFERENCES

(1) Fu, F.; Wang, Q. Removal of heavy metal ions from wastewaters: A review. *J. Environ. Manage.* **2011**, *92* (3), 407−418.
(2) Kilaru, H. V.; Ponnusamy, S. K.; Rames, C. P. A review on heavy metal pollution, toxicity and remedial measures: Current trends and future perspectives. *J. Mol. Liq.* **2019**, *290*, 111197 DOI: 10.1016/j.molliq.2019.111197.
(3) Muchuweti, M.; Birkett, J. W.; Chinyanga, E.; Zvauya, R.; Scrimshaw, M. D.; Lester, J. N. Heavy metal content of vegetables irrigated with mixtures of wastewater and sewage sludge in Zimbabwe: Implications for human health. *Agric. Ecosyst Environ.* **2006**, *112* (1), 41−48.
(4) Oyaro, N.; Juddy, O.; Murago, E. N. M.; Gitonga, E. The contents of Pb, Cu, Zn and Cd in meat in Nairobi Kenya. *Int. J. Food Agric. Environ.* **2007**, *5*, 119−121.
(5) Pawar, R. R.; Bajaj, H. C.; Lee, S. M. Activated bentonite as a low-cost adsorbent for the removal of Cu(II) and Pb(II) from aqueous solutions: Batch and column studies. *J. Ind. Eng. Chem.* **2016**, *34*, 213−223.
(6) Borba, C. E.; Guirardello, R.; Silva, E.A.; Veit, M.T.; Tavares, C. R. G. Removal of nickel(II) ions from aqueous solution by biosorption in a fixed bed column: Experimental and theoretical breakthrough curves. *BioChem. Eng.* **2006**, *30* (2), 184−191.
(7) Ghomi, M. A.; Moghaddam, J.; Ahmadi, N. P. A new approach to zinc−nickel separation using solution alkalinization method: application to a zinc plant residue. *Rare Met.* **2020**, *39*, 1341−1347.
(8) Jokar, M.; Mirghaffari, N.; Soleimani, M.; Jabbari, M. Preparation and characterization of novel bio ion exchanger from medicinal herb waste (chicory) for the removal of Pb^{2+} and Cd^{2+} from aqueous solutions. *J. Water Process Eng.* **2019**, *28*, 88−99.
(9) Xiang, X. L.; Bing, Y. J.; Xing, Y.; Hong, Y. M.; Ben, J. M. S. H. Highly permeable nanofibrous composite microfiltration membranes for removal of nanoparticles and heavy metal ions. *Sep. Purif. Technol.* **2020**; *233*, 115976 DOI: 10.1016/j.seppur.2019.115976.
(10) Hui, C. H. E. N.; Yonggang, L. U.; Dongxu, C. H. E. N. G.; Qun, Y. A. N. Synthesis and application in wastewater of a novel type of dithiocarbamate (DTC)-based heavy metal chelating agent. *J. Chin. J. Environ. Eng.* **2018**, *12*, 73.
(11) Xiang, B.; Fan, W.; Yi, X.; Wang, Z.; Gao, F.; Li, Y.; Gu, H. Dithiocarbamate-modified starch derivatives with high heavy metal adsorption performance. *J. Carbohydr. Polym.* **2016**, *136*, 30−37.
(12) Li, Q.; Yu, J.; Zhou, F.; Jiang, X.; et al. Synthesis and characterization of dithiocarbamate carbon nanotubes for the removal of heavy metal ions from aqueous solutions. *Colloids Surf. A* **2015**, *482*, 306−314.
(13) Shen, L. C.; Hankins, N. P.; Singh, R. Chapter 10-Surfactant and Polymer-Based Technologies for Water Treatment. Emerging Membr. Technol. *J. Sustainable Water Treat.* **2016**, 249−276.
(14) Tan, Z. D.; Zhang, H. Q. Synthesis and study of heavy metal ion capturing agent. *J. J. Hunan Eng. College.* 2014, *24*.
(15) Li, Q.; Yu, J.; Zhou, F.; Jiang, X.; et al. Synthesis and characterization of dithiocarbamate carbon nanotubes for the removal of heavy metal ions from aqueous solutions. *Colloids Surf. A* **2015**, *482*, 306−314.
(16) Li, J.; Wang, H. P.; Gao, Z. H.; et al. Study of DTC-modified polyurethane foam for trapping heavy metals. *J. Polyurethane Ind.* **2017**, *32*, 26−29.
(17) Masafumi, M., Iwakura, Kazuo, H. *Metal Seavengers for Wastewater[P]*. U. S. 1995; *2*, 7.
(18) Chen, H.; Qian, G.; Ruan, X.; Frost, R. L. Removal process of nickel(II) by using dodecyl sulfate intercalated calcium aluminum layered double hydroxide. *Appl. Clay Sci.* **2016**, *132*−*133*, 419−424.
(19) Liu, L.; Wu, J.; Li, X.; Ling, Y.; et al. Synthesis of poly (dimethyldiallylammonium chloride-co- acrylamide)-graft-triethylene-tetramine−dithiocarbamate and its removal performance and mechanism of action towards heavy metal ions. *Separation Purification Technol.* **2013**, *103*, 92−100.
(20) Petr, K. K.; Dmitry, S. V.; Olga, B. R.; Mikhail, A. P. FTIR photoacoustic spectroscopy for identification and assessment of soil components: Chernozems and their size fractions. *J. Photoacoust.* **2020**, *18*, 100162.
(21) Platero, E. E.; Mentruit, M. P.; Areán, C. O.; Zecchina, A. FTIR Studies on the Acidity of Sulfated Zirconia Prepared by Thermolysis of Zirconium Sulfate. *J. Catal.* **1996**, *162* (2), 268−276.
(22) Chen, G. Y.; Hao, D.; Yuan, Y. Q.; Ming, X. L.; Bing, C.; Zhen, Y. X.; Rui, F. K. Absorption lines measurements of carbon disulfide at 4.6 μm with quantum cascade laser absorption spectroscopy. *Spectrochim. J. Acta, Part A* **2020**, *225*, 117478.
(23) Koshy, K. M.; Boggs, J. M. The effect of anomerism and hydration on the C-O-S vibrational frequency of d-galactose-3-sulfate determined by FTIR spectroscopy. *Carbohydr. Res.* **1997**, *297* (2), 93−99.
(24) Mehmet, E. A.; Şukru, D. Removal of heavy metal ions using chemically modified adsorbents. *J. Environ. Appl. Sci.* **2006**, *1*, 27−40.
(25) Heidari, A.; Younesi, H.; Mehraban, Z. Removal of Ni(II), Cd(II), and Pb(II) from a ternary aqueous solution by amino functionalized mesoporous and nano mesoporous silica. *Chem. Eng. J.* **2009**, *153* (1−3), 70−79.
(26) Ngomsik, A. F.; Bee, A.; Siaugue, J. M.; Talbot, D.; Cabuil, V.; Cote, G. Co(II) removal by magnetic alginate beads containing Cyanex 272. *J. Hazard. Mater.* **2009**, *166* (2−3), 1043−1049.
(27) Dehghani, M. H.; Sarmadi, M.; Alipour, M. R.; Sanaei, D.; Abdolmaleki, H.; Agarwal, S.; Gupta, V. K. Investigating the equilibrium and adsorption kinetics for the removal of Ni (II) ions from aqueous solutions using adsorbents prepared from the modified waste newspapers: A low-cost and available adsorbent. *Microchemical. J.* **2019**, *146*, 1043−1053.
(28) Ouyang, Q.; Kou, F.; Zhang, N.; Lian, J.; Tu, G.; Fang, Z. Tea polyphenols promote Fenton-like reaction: pH self-driving chelation and reduction mechanism. *Chem. Eng. J.* **2019**, *366*, 514−522.
(29) Chen, J.; Hao, Y.; Chen, M. Rapid and efficient removal of Ni^{2+} from aqueous solution by the one-pot synthesized EDTA-modified magnetic nanoparticles. *Environ. Sci. Pollut Res.* **2014**, *21*, 1671−1679.
(30) Lin, S. T.; Tran, H. N.; Chao, H. P.; Lee, J. F. Layered double hydroxides intercalated with sulfur-containing organic solutes for efficient removal of cationic and oxyanionic metal ions. *Appl. Clay Sci.* **2018**, *162*, 443−453.
(31) Huang, R.; Shao, N.; Hou, L.; Zhu, X. Fabrication of an efficient surface ion-imprinted polymer based on sandwich-like graphene oxide composite materials for fast and selective removal of lead ions. *Colloids Surf. A* **2019**, *566*, 218−228.
(32) Yurlova, L.; Kryvoruchko, A.; Kornilovich, B. Removal of Ni(II) ions from wastewater by micellar-enhanced ultrafiltration. *Desalination.* **2002**, *144*, 255−260.
(33) Du, J.; Zhang, C. An overview of the research progress of low-cost adsorbents for the treatment of heavy metal-containing wastewater. *J. Comprehensive Util. Fly Ash.* **2006**, *05*, 49−52.
(34) Wang, K. J. *Study on the treatment of lead tannate wastewater by adsorption precipitation advanced oxidation method*. North Central University: D. Taiyuan. 2017.
(35) Yi, Y. R.; Zheng, M.; Du, Y. C. Experimental study on the purification of lead-containing wastewater by fly ash adsorption. *J. Environmental Monitoring Management and Technology.* **2018**, *30* (2), 20−24.
(36) Wang, Z. H.; Tao, S. J.; Yu, F. J.; et al. Modification of natural zeolite and its adsorption of Pb^{2+} and Cu^{2+}. *J. Northeastern Univ.* **2012**, *33* (11), 16−37.
(37) Sven, S. L. K. About the theory of so-called adsorption of soluble substances. *J. Handl.* **1898**, *24*, 1−39.
(38) Ho, Y. S.; Wase, D. A. J.; Forster, C. F. Removal of lead ions from aqueous solution using sphagnum moss peat as adsorbent. *J. Water SA.* **1996**, *22*, 219−224.
(39) Brito, M. J. P.; Veloso, C. M.; Santos, L. S.; Bonomo, R. C. F.; Fontan, R. D. C. I. Adsorption of the textile dye Dianix royal blue CC

https://doi.org/10.1021/acsomega.3c05476
ACS Omega 2023, 8, 41512−41522

onto carbons obtained from yellow mombin fruit stones and activated with KOH and H_3PO_4: kinetics, adsorption equilibrium and thermodynamic studies. *J. Powder Technol.* **2018**, *339*, 334−343.
(40) Moussout, H.; Ahlafi, H.; Aazza, M.; Maghat, H. Critical of linear and nonlinear equations of pseudo-first order and pseudo-second order kinetic models. *Karbala Int. J. Modern Sci.* **2018**, *4*, 244−254.
(41) Li, H. L.; Si, Y. L.; Hong, L. P.; Zheng, C. Y.; Lu, Z.; An, P. T. Surface charge of mesoporous calcium silicate and its adsorption characteristics for heavy metal ions. *J. Solid State Sci.* **2020**, *99*, 106072.
(42) Liu, Y.; Hu, L.; Tan, B.; Li, J.; Gao, X.; He, Y.; Du, X.; Zhang, W.; Wang, W. Adsorption behavior of heavy metal ions from aqueous solution onto composite dextran-chitosan macromolecule resin adsorbent. *Int. J. Biol. Macromol.* **2019**, *141*, 738−746.
(43) Nieboer, E.; Richardson, D. H. S. The replacement of the nondescript term 'heavy metals' by a biologically and chemically significant classification of metal ions. *J. Environ. Pollut. Series B, Chem. Phys.* **1980**, *1* (1), 3−26.
(44) Marina, M.; Vladimir, I.; Natalia, Y.; Lidia, G. The effect of heavy metal ions hydration on their sorption by a mesoporous titanium phosphate ion-exchanger. *J. Water. Process. Eng.* **2020**, *35*, 101233.
(45) Jian, H. Q.; Xue, T.; Zhao, J.; Bo, C.; Modupe, S. A.; Qi, H.; Cheng, C. F.; Yan, F.; Xian, L. M.; Ying, Z. Multi-component adsorption of Pb(II), Cd(II) and Ni(II) onto microwave function-alized cellulose: Kinetics, isotherms, thermodynamics, mechanisms and application for electroplating wastewater purification. *J. Hazard. Mater.* **2020**, *387*, 1166.
(46) Ren, H.; Gao, Z.; Wu, D.; Jiang, J.; Sun, Y.; Luo, C. Efficient Pb(II) removal using sodium alginate−carboxymethyl cellulose gel beads: Preparation, characterization, and adsorption mechanism. *Carbohydr. Polym.* **2016**, *137*, 402−409.
(47) Shen, F.; Su, J.; Zhang, X.; Zhang, K.; Qi, X. Chitosan-derived carbonaceous material for highly efficient adsorption of chromium (VI) from aqueous solution. *Int. J. Biol. Macromol.* **2016**, *91*, 443−449.
(48) Wondracek, M. H. P.; Jorgetto, A. O.; Silva, A. C. P.; Ivassechen, J. d. R.; Schneider, J. F.; Saeki, M. J.; Pedrosa, V. A.; Yoshito, W. K.; Colauto, F.; Ortiz, W. A.; Castro, G. R. Synthesis of mesoporous silica-coated magnetic nanoparticles modified with 4-amino-3-hydrazino-5-mercapto-1,2,4-triazole and its application as Cu(II) adsorbent from aqueous samples. *J. Appl. Surface Sci.* **2016**, *367*, 533−541.
(49) Yeong, Y. C.; Jong, H. B.; Yohei, H.; Sol, A.; Ick, S. K.; Hoik, L.; Myungwoong, K. Thiol-functionalized cellulose nanofiber membranes for the effective adsorption of heavy metal ions in water. *J. Carbohydr. Polym.* **2020**, *234*, 115881.
(50) Xiang, B.; Fan, W.; Yi, X.; Wang, Z.; Gao, F.; Li, Y.; Gu, H. Dithiocarbamate-modified starch derivatives with high heavy metal adsorption performance. *J. Carbohydr. Polym.* **2016**, *136*, 30−37.
(51) Li, B.; Guo, J. Z.; Liu, J. L.; Fang, L.; Lv, J. Q.; Lv, K. Removal of aqueous-phase lead ions by dithiocarbamate-modified hydrochar. *J. Sci. Total Environ.* **2020**, *714*, 136897.
(52) Xia, B. *Study on the removal, recovery and application of Mn2+ in water by TiO2 photocatalytic system*. D. Guangdong University of Technology, 2022.
(53) Huang, S.; Gu, L.; Zhu, N.; Feng, K.; Yuan, H.; Lou, Z.; Li, Y.; Shan, A.; et al. Heavy metal recovery from electroplating wastewater by synthesis of mixed-Fe3O4@SiO2/metal oxide magnetite photo-catalysts. *Green Chem.* **2014**, *16* (5), 2696−2705.

https://doi.org/10.1021/acsomega.3c05476
ACS Omega 2023, 8, 41512−41522